

Full length article

# Polyaspartic acid as a corrosion inhibitor for WE43 magnesium alloy

Lihui Yang\*, Yantao Li, Bei Qian, Baorong Hou

*Institute of Oceanology, Chinese Academy of Sciences, Qingdao, 266071, China*

Received 19 September 2014; revised 20 December 2014; accepted 25 December 2014

Available online 24 March 2015

## Abstract

The inhibition behavior of polyaspartic acid (PASP) as an environment-friendly corrosion inhibitor for WE43 magnesium alloy was investigated in 3.5 wt.% NaCl solution by means for EIS measurement, potentiodynamic polarization curve, and scanning electron microscopy. The results show that PASP can inhibit the corrosion of WE43 magnesium alloy. The maximum inhibition efficiency is achieved when PASP concentration is 400 ppm in this study.

Copyright 2015, National Engineering Research Center for Magnesium Alloys of China, Chongqing University. Production and hosting by Elsevier B.V. All rights reserved.

**Keywords:** Magnesium alloy; Polyaspartic acid; Inhibitor; Corrosion

## 1. Introduction

Magnesium alloys have recently attracted more and more attention for their unique physical and chemical properties, including light weight, high strength-to-weight ratio, excellent damping behavior, good electromagnetic shielding, satisfactory castability, and wonderful recyclability [1–6]. However, magnesium alloys have some undesirable properties, such as the high chemical reactivity and poor corrosion resistance that have hindered their use in many applications [7].

Inhibitor is one of the most practical corrosion protection methods for protecting metals and alloys from corrosion attack. Corrosion inhibitors have been extensively studied on steel, aluminum alloys, and copper substrates [8–13]. Recently there are also a few publications about directly using corrosion inhibitors in solution to protect magnesium alloys [14–20]. However, the main challenge is the lack of high efficiency inhibitors. Also many corrosion inhibitors have

some health and/or environmental problems due to their toxicity. It is highly desired that new inhibitors for Mg are non-toxic and environment-friendly.

PASP has been synthesized and used as one of the green water treatment agents [21,22]. There are several researches on the inhibition of PASP for carbon steel [9]. However, there are few reports on the corrosion inhibition behavior of PASP on magnesium alloys in sodium chloride solutions.

In the present work, the inhibition behavior of PASP as an environment-friendly corrosion inhibitor for WE43 magnesium alloy was investigated. EIS measurement, Potentiodynamic polarization and SEM were employed to study the effect of different concentration of PASP.

## 2. Experimental

### 2.1. Material and solution

The substrate material used was WE43 alloy (4 wt.%Y, 3 wt.%Nd, 0.5%Zr and Mg balance) with a size of 10 mm × 10 mm × 3 mm. Specimens were abraded with 2000<sup>#</sup> SiC paper to obtain an even surface, ultrasonically cleaned using acetone and washed with an alkaline detergent.

\* Corresponding author.

E-mail address: [ylhheu@163.com](mailto:ylhheu@163.com) (L. Yang).

Peer review under responsibility of National Engineering Research Center for Magnesium Alloys of China, Chongqing University.

The chemical structure of the used polyaspartic acid (PASP) is shown in Fig. 1. PASP was prepared by thermal condensation reaction of L-aspartic acid. The synthesized PASP was characterized by Fourier transform infrared (FTIR). FTIR spectroscopy was performed using the Bruker Vertex 70 FT-IR. Spectra were collected from 16 scans at a resolution of  $4\text{ cm}^{-1}$  between  $400\text{ cm}^{-1}$  and  $4000\text{ cm}^{-1}$ .

## 2.2. Electrochemical measurements

To evaluate the corrosion performance and possible behavior of the samples, electrochemical measurements were performed on an electrochemical analyzer (IM6ex, Zahner, Germany). Potentiodynamic polarization was conducted in neutral 3.5 wt.% NaCl aqueous solution at room temperature. A standard three-compartment cell was used with a saturated calomel electrode (SCE) and a platinum electrode as a reference and counter electrode, respectively. All of the electrodes were cleaned in acetone agitated ultrasonically, rinsed in deionized water before the electrochemical tests. The coated samples were masked with epoxy resins so that only  $1\text{ cm}^2$  area was exposed to the electrolyte. During the potentiodynamic sweep experiments, the samples were first immersed into electrolyte for 10 min to stabilize the OCP. The sweeping rate was  $1\text{ mV/s}$  for all measurements. Electrochemical impedance spectroscopy (EIS) was performed in frequency range from  $10\text{ kHz}$  to  $10\text{ mHz}$ . The obtained EIS data points were fitted using commercial software ZsimpWin.

## 2.3. SEM

Surface morphologies of the magnesium samples were observed by SEM (JSM- 6480A, Japan Electronics) instrument before and after the immersion of samples in both the inhibited and the blank acid solutions.

## 3. Results and discussion

### 3.1. FTIR of PASP

Fig. 2 shows the FTIR spectra of the synthesized PASP. The absorption bands appear at  $1190\text{ cm}^{-1}$  and  $3411\text{ cm}^{-1}$  correspond to the C–O and O–H, which is the major band of –COOH. Peak at  $1390\text{ cm}^{-1}$  is related to the C–N stretching mode of the acylamide group. The peak at  $1600\text{ cm}^{-1}$  is

assigned to the bending of N–H. The results indicate that the PASP is successfully synthesized.

### 3.2. Electrochemical impedance spectroscopy (EIS) measurements

Fig. 3 shows the EISs of WE43 magnesium alloy in the blank and PASP containing solutions at room temperature. Two electrochemical equivalent circuits shown in Fig. 4 are used to fit the different EIS plots. Fig. 4a shows the circuit for an uninhibited WE43 magnesium alloy surface, and Fig. 4b shows a circuit which simulates a WE43 magnesium surface with inhibitor deposits blocking the active corrosion sites.  $R_s$  represents the solution resistance;  $CPE_1$  is the constant phase element related to the surface film formed on WE43;  $R_f$  is the resistance of the protective-film;  $CPE_2$  is also a constant phase element representing the double layer capacitance of the metal/solution interface and  $R_{ct}$  is the charge transfer resistance of the interface.  $L$  is the inductance, and  $W$  is the spreading resistance. The parameters derived from EIS curve fitting are listed in Table 1.

The polarization resistance,  $R_p = R_f + R_{ct}$ , can be used to evaluate the inhibition efficiency:

$$\eta (\%) = \frac{R_p^i - R_p^0}{R_p^i} \times 100\%$$

where  $R_p^0$  and  $R_p^i$  are polarization resistances in the solution without and with a PASP containing, respectively. The estimated inhibition efficiencies are also listed in Table 1. It can be seen that the best performance efficiency of PASP on WE43 magnesium alloy was 94.2%, which took place in  $400\text{ ppm}$  concentration.

### 3.3. Potentiodynamic polarization curve tests

Fig. 5 shows the polarization curves of samples in different concentrations of PASP solutions. It can be seen that for the WE43 Mg substrate, both cathodic and anodic branches exhibit an active response which suggesting a poor corrosion resistance. For samples, in different concentrations of PASP solution, the corrosion potential shifts towards the noble direction and the corrosion current density decreased. This indicates the increase of the corrosion resistance. However, with the presence of the passivation region, Tafel slopes are not clear in Fig. 5 and Tafel

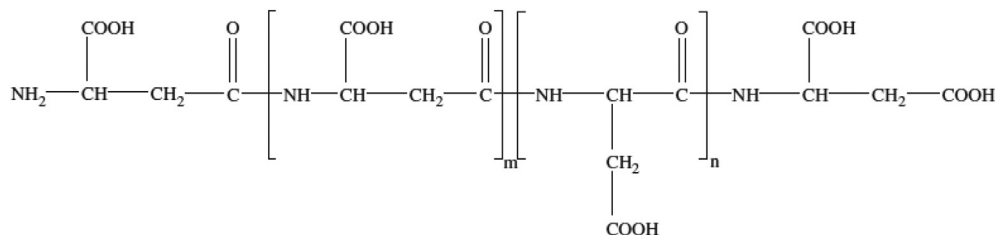


Fig. 1. Chemical structure of PASP repeat unit.

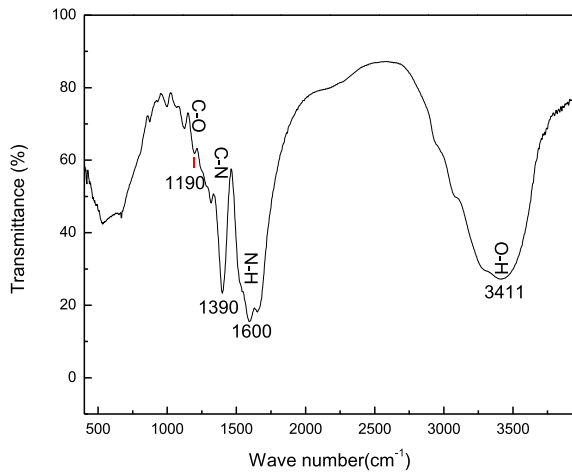


Fig. 2. FTIR of synthesized PASP.

method is not fit to analyze the polarization curves. However, as a complement to the EIS tests, the polarization tests confirm that PASP could act as a good corrosion inhibitor for protecting WE43 magnesium alloy from corrosion.

### 3.4. Morphological studies

Fig. 6 shows the surface morphology of the WE43 Mg alloy samples after 3 days of immersion in 3.5 wt.% NaCl blank solution and that with various PASP concentrations. As shown in Fig. 6(a), the metal surface was covered with corrosion products. When the PASP is added in the solution, there is a protective film formed by adsorption of PASP on the metal surface. Non-penetrating cracked morphology with leaf-like microstructure existed on these films, which is very similar with that of chemical conversion coatings [23]. The film is the most compact when the

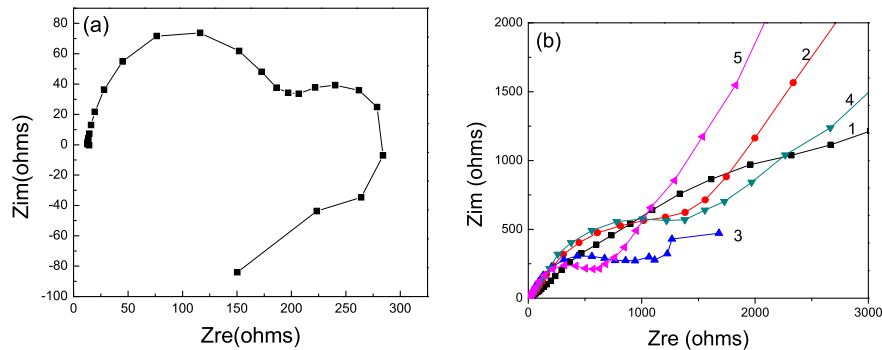


Fig. 3. EISs of WE43 in 3.5% NaCl solution without or with PASP(a) blank; (b) with different concentration PASP(1–5):400 ppm; 600 ppm; 800 ppm; 1200 ppm; 2000 ppm.

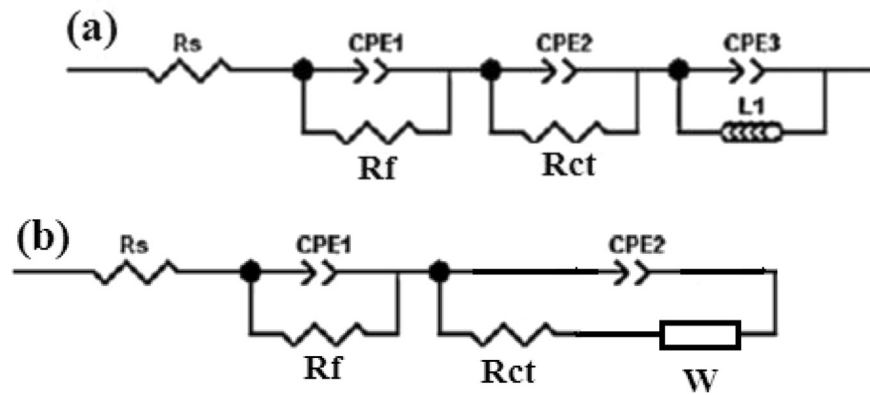


Fig. 4. Equivalent circuit for WE43 magnesium alloy in 3.5 wt.% NaCl solutions without and with PASP.

Table 1

Inhibition efficiencies based on EIS measurements and electrochemical parameters obtained from the measured EISs of WE43 magnesium alloy in 3.5 wt.% NaCl blank solution and PASP containing solutions.

PASP concentration (g/L)	$R_s$ ( $\Omega\text{cm}^2$ )	$CPE_1$ ( $\text{Fcm}^{-2}$ )	$R_f$ ( $\Omega\text{cm}^2$ )	$CPE_2$ ( $\text{Fcm}^{-2}$ )	$n$	$R_{ct}$ ( $\Omega\text{cm}^2$ )	$W$ ( $\Omega\text{cm}^2$ )	Inductance (H)	$\eta$ (%)
0	13.71	$2.234 \times 10^{-5}$	157.9	0.001956	—	85.43	—	94.73	—
0.4	19.79	$3.673 \times 10^{-7}$	14.24	0.000174	0.4496	4169	0.0008946	—	94.2
0.6	19.89	$4.332 \times 10^{-5}$	538.9	0.0001311	0.5644	585.6	0.0004763	—	78.4
0.8	14	$5.958 \times 10^{-5}$	169.5	0.00016	0.6473	908.9	0.004008	—	77.4
1.2	13.44	$2.566 \times 10^{-5}$	505.6	0.0002289	0.4915	2433	0.0006575	—	91.7
2.0	12.75	$3.666 \times 10^{-5}$	293.6	0.0001796	0.6231	257.1	0.001325	—	55.8

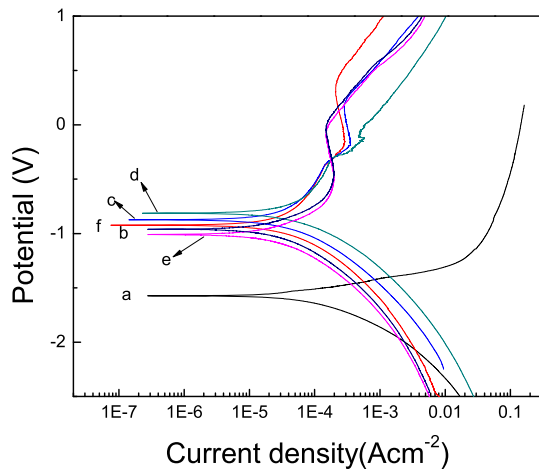


Fig. 5. Potentiodynamic polarization curves for WE43 alloy in the blank solution and PASP containing solution at 25 °C (a) blank; (b–f) with different concentration PASP: 400 ppm; 600 ppm; 800 ppm; 1200 ppm; 2000 ppm.

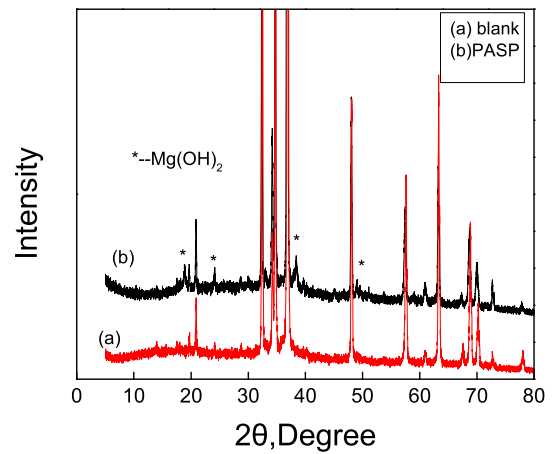


Fig. 7. XRD patterns of WE43 magnesium alloy before (a) and after PASP solutions immersion (b).

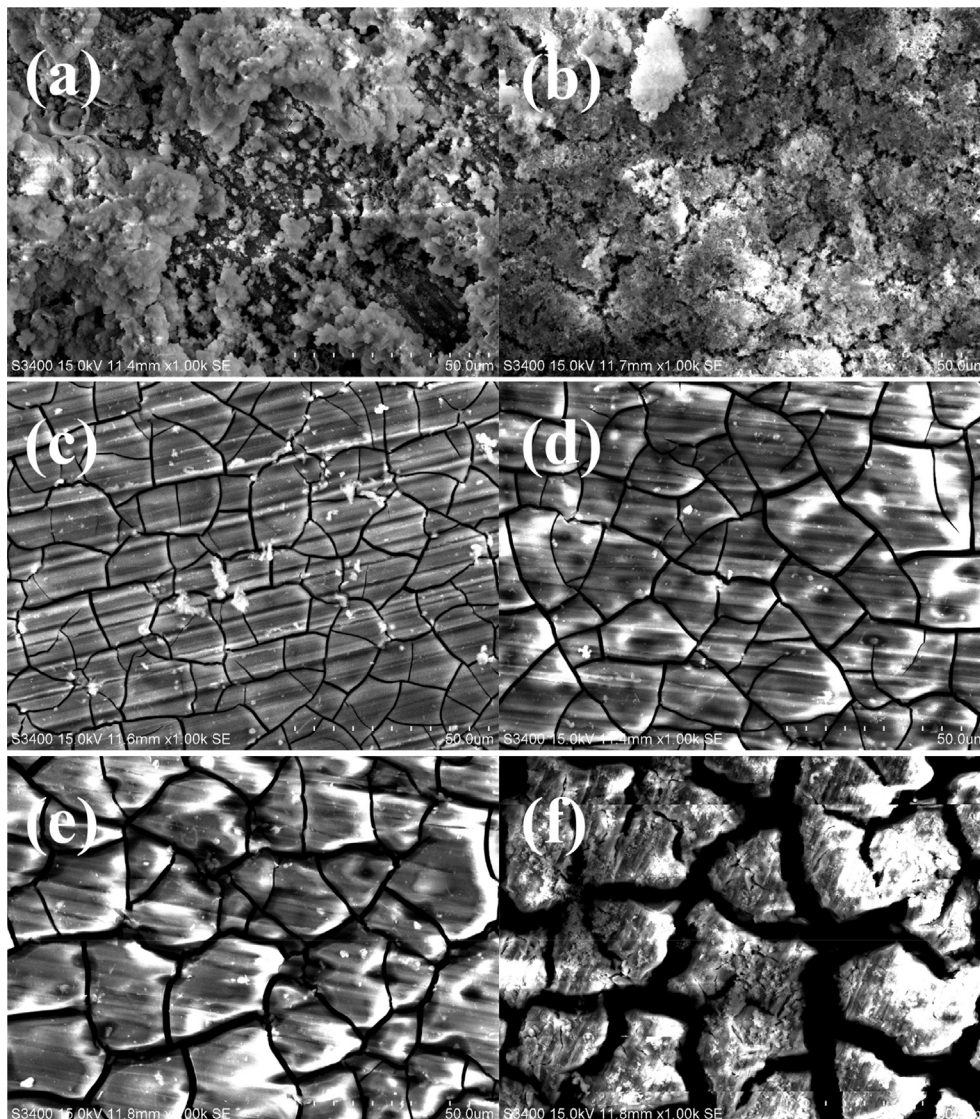


Fig. 6. SEM images of WE43 magnesium alloy after 3 days of immersion in 3.5 wt.% NaCl blank solution (a), and that with various PASP concentrations: b-400 ppm; c-600 ppm; d-800 ppm; e-1200 ppm and f-2000 ppm.

PASP concentration is 400 ppm. The protective nature of the film formed on the WE43 magnesium alloy is confirmed by both SEM examination and electrochemical methods.

### 3.5. Inhibition mechanism

Fig. 7 shows the XRD patterns of WE43 magnesium alloy before (a) and after PASP solutions immersed. It is noted that there are some new peaks appeared corresponding to  $\text{Mg}(\text{OH})_2$ . There maybe some other compositions which cannot be detected by XRD. We suppose that When PASP is added to the NaCl solution, PASP anions get into some relatively large pores of the  $\text{Mg}(\text{OH})_2$  surface film, and chelate directly with the  $\text{Mg}^{2+}$  ions dissolved from the substrate Mg alloy in the film pores, forming PASP–Mg complex precipitated in the pores. The deposited PASP–Mg complex products seal the film pores to a great degree. The best corrosion protection is offered by a surface film with  $\text{Mg}(\text{OH})_2$  and PASP–Mg mixed at a certain ratio.

## 4. Conclusions

PASP was synthesized by a simple thermal condensation reaction method starting from L-aspartic acid and was confirmed by FTIR analysis to detect the existence of characteristic functional groups.

PASP has presented a good inhibitory action and a significant efficiency for decreasing the corrosion rate of the studied magnesium alloys. The inhibition efficiency was found to increase by increasing the PASP concentration; the best performance efficiency of PASP on WE43 magnesium alloy was 94.2%, which took place in 400 ppm concentration. Potentiodynamic polarization results revealed that in different concentrations of PASP solution the corrosion potential shifts towards the noble direction and the corrosion current density decreased, which indicates the increase of the corrosion resistance. SEM displays that there are protective films formed on the surface in different concentrations of PASP solution.

## Acknowledgment

The authors gratefully acknowledge the financial support of the National Natural Science Foundation of China (No. 41276074) and National Basic Research Program of China (No. 2014CB643304).

## References

- [1] E. Ghali, *Magnesium and Magnesium Alloys*, Uhlig's Corrosion Handbook, 2000, pp. 793–830.
- [2] M.M. Avedesian, H. Baker, *ASM Specialty Handbook: Magnesium and Magnesium Alloys*, 1999.
- [3] G.L. Song, Z. Xu, *Corros. Sci.* 54 (2012) 97–105.
- [4] Z. Pu, G.L. Song, S. Yang, et al., *Corros. Sci.* 57 (2012) 192–201.
- [5] G.L. Song, R. Mishra, Z. Xu, *Electrochem. Commun.* 12 (2010) 1009–1012.
- [6] Y.W. Song, D.Y. Shan, R.S. Chen, et al., *Corros. Sci.* 52 (2010) 1830–1837.
- [7] G. Ballerini, U. Bardi, R. Bignucolo, et al., *Corros. Sci.* 47 (2005) 2173–2184.
- [8] N.D. Nam, Q.V. Bui, M. Mathesh, et al., *Corros. Sci.* 76 (2013) 257–266.
- [9] B. Qian, J. Wang, M. Zheng, et al., *Corros. Sci.* 75 (2013) 184–192.
- [10] M. Whelan, K. Barton, J. Cassidy, et al., *Surf. Coat.* 242 (2013) 86–90.
- [11] M.M. Fares, A.K. Maayta, M.M. Al-Qudah, *Corros. Sci.* 60 (2012) 112–117.
- [12] Matjaž Finšgar, *Corros. Sci.* 77 (2013) 350–359.
- [13] Z.Y. Chen, L. Huang, G.A. Zhang, et al., *Corros. Sci.* 65 (2012) 214–222.
- [14] J.Y. Hu, D.Z. Zeng, Z. Zhang, et al., *Corros. Sci.* 74 (2013) 35–43.
- [15] J.Y. Hu, D. B. Huang, G.L. Song, et al., *Corros. Sci.* 53 (2011) 4093–4101.
- [16] D. Seifzadeh, H. Basharnavaz, *Trans. Nonferrous Met. Soc. China* 23 (2013) 2577–2584.
- [17] H. Gao, Q. Li, Y. Dai, F. Luo, et al., *Corros. Sci.* 52 (2010) 1603–1609.
- [18] A. Mesbah, C. Juers, G.A. Zhang, et al., *Solid State Sci.* 9 (2007) 322–328.
- [19] J.Y. Hu, D.B. Huang, G.A. Zhang, et al., *Corros. Sci.* 63 (2012) 367–378.
- [20] H. Gao, Q. Li, F.N. Chen, et al., *Corros. Sci.* 53 (2011) 1401–1407.
- [21] M. Tomida, T. Nakato, S. Matsunami, et al., *Polymer* 38 (1997) 4733–4736.
- [22] Dorota Kołodźńska, *Chem. Eng. J.* 173 (2011) 520–529.
- [23] H. Zhang, G.C. Yao, S.L. Wang, et al., *Surf. Coat. Technol.* 202 (2008) 1825–1830.